Journal of Oil Palm Research Vol. 29 (2) June 2017 p. 278 – 290

ACTIVATED CARBON FROM OIL PALM BIOMASS AS POTENTIAL ADSORBENT FOR PALM OIL MILL EFFLUENT TREATMENT

NUR SULIHATIMARSYILA ABD WAFTI*; HARRISON LIK NANG LAU*; SOH KHEANG LOH*; ASTIMAR ABDUL AZIZ*; ZULKIFLI AB RAHMAN* and CHOO YUEN MAY**

ABSTRACT

The study aims to produce renewable and green activated carbon (AC) from palm biomass through pyrolysis and the activation process. The study also aims to evaluate the application of AC as adsorbent in palm oil mill effluent treatment (POME). This is in order to reduce the pollutant levels in its final discharge. The AC was prepared from empty fruit bunch (EFB), by pyrolysis (to produce bio-char), followed by physical activation. The bio-chars with higher carbon content were selected for the preparation of the AC. The physical activation process was carried out by purging with carbon dioxide (100 cm^3 min^{-1}) at 10°C min^{-1} heating rate for 30 min until the AC reaches the desired activation temperature. The activation temperatures studied ranged from 500°C to 900°C in quartz tube furnace. The optimum activation temperature i.e. *800°C gave the maximum specific surface area, (S_{BET}) of 937 m^2 g^{-1}. Batch adsorption experiments applying the prepared adsorbent to synthetic dye yielded adsorption data well fitted to the Langmuir isotherm model. The AC produced from EFB performed better in dye removal achieving a maximum adsorption capacity of 333.3 mg g^{-1}. The EFB-based AC was able to reduce the biochemical oxygen demand of POME. These studies suggested that the EFB AC could be useful as a low cost alternative adsorbent in wastewater treatment.*

Keywords: oil palm, empty fruit bunch, biochar, physical activation, adsorption isotherm, palm oil mill effluent.

Date received: 3 March 2017; **Sent for revision:** 8 March 2017; **Received in final form:** 11 April 2017; **Accepted:** 27 April 2017.

INTRODUCTION

In palm oil milling, about 5%-7% palm kernel shell (PKS), 21%-22% empty fruit bunch (EFB) and 12%-16% mesocarp fibre (MF) are generated from each tonne of fresh fruit bunch (FFB) processed (Loh, 2016). In 2015, the Malaysian palm oil mills processed about 98.34 million tonnes of FFB (MPOB, 2015). Hence, an estimated 4.56 million tonnes of PKS, 21.63 million tonnes of EFB and 15.73 million tonnes of MF were available as by-products.

Activated carbon (AC) is well-known for its capability to remove impurities, *e.g.* harmful chemicals in either liquid or gas phase. It is an amorphous form of carbon having a very large surface area ranging from about 500 to 1500 m^2 g^{-1} with a highly developed internal pore structure. Basically, the AC can be produced from natural feedstocks such as woods (Michael, 1996), shells (Aygun *et al*., 2003), bamboos (Hameed *et al*., 2007), corns (Freel *et al*., 2004), date pits (Banat *et al*., 2003)

* Malaysian Palm Oil Board, 6 Persiaran Institusi, Bandar Baru Bangi, 43000 Kajang, Selangor, Malaysia. E-mail: nursulihati@mpob.gov.my

** Malaysian Oil Scientists' and Technologists' Association, C3 A-10, 4th Floor, Damansara Intan, 1 Jalan SS 20/27, 47400 Petaling Jaya, Selangor, Malaysia.

and soyabean oil cake (Tay *et al*., 2009). Although oil palm biomass is renewable and potentially less expensive than other materials to produce AC, much of the past research has thus far focused on PKS (Jumasiah *et al*., 2005; Guo and Lua, 2001; 2002; Guo *et al*., 2005; 2008; Daud *et al*., 2000; Yacob *et al*., 2008). Being naturally soft, the EFB fibre has received less attention. Nevertheless, with proper pre-treatment and activation, EFB could be one of the alternatives to produce AC successfully and sustainably.

AC are produced by carbonising suitable raw materials to enhance the carbon content and create an initial porosity in the resulting char materials. The selection of carbonisation parameters particularly the temperature is critical as it affects the structure and the desired quality of the AC produced. High carbonisation temperature would result in a greater amount of volatiles being released from the raw material and influences the product yield and porosity. Activation process further develops the porosity of the carbonised materials by creating some orders of the pore structures to the final product. These pores can be classified according to the International Union of Pure and applied Chemistry (IUPAC) as micropores (width, d< 2 nm), mesopores (2 nm<d<50 nm) and macropores (d>50 nm) (Gregg and Sing, 1982). The size of pores will have an effect on the porosity and total surface area of the AC that is made available for adsorption.

The activation process can be accomplished by either chemical or physical activation. The former is created by dehydration reactions at low temperatures with chemical agents such as phosphoric acid (Guo and Lua, 2002; Tiryaki *et al*., 2014), potassium hydroxide (Foo and Hameed, 2011a) and zinc chloride (Hu and Srinivasan, 2000) whereas the latter employs carbon dioxide or steam as oxidising agents at higher temperatures. The physical process is more commonly used in the production of AC with temperature ranging from 600°C-1200°C (Bouchelta *et al*., 2008; Ismadji *et al*., 2005; Arenas and Chejne, 2004).

Many studies have revealed the application of AC in adsorption. Gueye *et al*. (2014) found that AC from jatropha wood was more efficient than AC produced from peanut shells for the removal of Cr(VI) from wastewater contaminated by toxic pollutants. Sekirifa *et al.* (2013) presented interesting adsorptive properties on the AC produced from date stones under physical activation. Treviño-Cordero *et al.* (2008) showed that AC produced from plum kernel performed better as a potential adsorbent for the removal of heavy metals such as lead (Pb^{2+}) and dyes such as acid blue and methylene blue (MB) from wastewater compared to jacaranda fruit AC. Nunes *et al.* (2009) revealed that AC from coffee press cake had great potential as an inexpensive alternative adsorbent for dyes removal in wastewater treatment.

In the case for oil palm biomass, PKS was found convertible into AC by thermal physical activation (Guo and Lua, 2001; Daud *et al*., 2000; Tan *et al*., 2008) and chemical activation (Adinata *et al*., 2007; Hayashi *et al*., 2002). The PKS AC produced was evaluated on its capability to adsorb basic dye from aqueous solution (Jumasiah *et al*., 2005). On the other hand, Osman *et al*. (2016) studied the production of AC from the core and shaggy part of oil palm EFB. The AC from EFB was produced via the pyrolysis process at 450°C followed by the physical activation process at the desired temperature from 600°C to 800°C under CO_2 flow with different time of activation of 30, 60 and 120 min. The study showed that the highest yield of AC was obtained at 700°C and 30 min holding time. Astimar and Deraman (2013) prepared carbon granules from EFB via a slow pyrolysis process at 280°C under vacuum followed by sulphuric acid (H_2SO_4) treatment prior to carbonisation at 600°C-800°C under nitrogen flow. The study showed that H_2SO_4 and carbonisation temperature could significantly affect the quality of the AC in terms of porosity and micro-structure. Hameed *et al*. (2009) revealed that the physical properties, *i.e.* specific surface area, total pore volume and average pore diameter of the EFB-based AC under chemical-physical activation were >1000 m^2 g^{-1}, 0.6 cm^3 g^{-1} and 2.5 nm, respectively, indicating that the AC was a mesopore adsorbent. Subsequently it was shown to be a promising low cost adsorbent in contaminants (phenol/MB) removal from aqueous solution. Siti Hadjar *et al*. (2012) showed that EFB-based AC prepared from CO_2 activation had better phenol adsorption capacity as compared to the commercial AC. The kinetics of direct phenol adsorption of AC followed the pseudo-second order model; and the equilibrium data fitted well with the Langmuir isotherm (Adinata *et al*., 2007). The adsorption isotherms and desorption of 2,4,6-trichlorophenol (TCP) as adsorbate on EFB AC showed that it was a promising low cost adsorbent (Tan *et al*., 2009). Md Arshad *et al*. (2016) produced the AC from EFB which were activated using physical and chemical processes. The AC has been tested on its hydrogen storage capacity. The surface area (S_{BET}) and microporous structures of the AC produced were in the range of 305-687 m^2 g^{-1} and up to 94%, respectively. The high S_{BET} and well-developed microporous carbon materials are necessary in enhancing the hydrogen adsorption capacity.

Mubarak *et al.* (2016) investigated the conversion of EFB to biochar using microwave-assisted heating. The surface properties including S_{BET} and pore volume of biochar were enhanced. The study also compared the conventional heating method with the microwave-assisted method. It was found that the conventional method gave a long activation process compared to the shorter

activation process in the microwave irradiation method. Oil palm EFB can also be pyrolysed using microwave-assisted irradiation and the results showed that the characteristic in terms of fuel and chemical characteristic of EFB are comparable to other biomasses (Omar *et al*., 2011).

Nor Faizah *et al*. (2017) investigated the application of PKS AC in reducing the pollutants in POME as an alternative treatment system. The AC was obtained from a carbonisation system which has a low S_{BET} of 566.27 m^2 g^{-1}. The study found that the AC with high dosages and long treatment time was able to remove the organic pollutant and the coloured compound in POME. Hence, the activation process has helped enhance the adsorption capability of organic pollutant compound. Amosa (2015) produced EFB-based powdered AC from carbonisation and steam activation to be applied in the treatment of POME. The AC with high S_{BET} of 886 m^2 g^{-1} gave better adsorption efficiency removals for manganese (Mn) and hydrogen sulphide (H_2S). The EFB-based AC could be utilised as a standard adsorbent to replace the expensive adsorbent in wastewater treatment system.

Previous studies have evaluated the adsorption capability of the prepared AC using artificial pollutants such as MB (Foo *et al*., 2011b; Hameed *et al*., 2007), sulphur dioxide (Guo and Lua, 2002), iodine (Ceyhan *et al*., 2013) and phenol (Alam *et al*., 2009). A few papers evaluated the AC adsorption capability using actual industrial wastewater treatment (Masoud *et al*., 2016; Malik, 2004; Devi *et al*., 2008; Zahrim *et al*., 2009). Having reviewed all the potentials to convert oil palm biomass into AC, this study attempted producing AC from EFB via pyrolysis and the physical activation processes and investigated its suitability in POME treatment. The study exploited the possibility of utilising the abundantly available oil palm biomass to treat POME in a sustainable way.

MATERIALS AND METHODS

Materials

Various oil palm biomass samples (EFB, PKS, MF) were obtained from the Malaysian Palm Oil Board Palm Oil Mill Technology Centre (POMTEC), Labu, Negeri Sembilan, Malaysia. *Table 1* shows the proximate and ultimate analyses of the oil palm biomass used. *Table 2* shows the surface characteristics of the oil palm biomass samples evaluated by nitrogen adsorption-desorption study at -196°C [Accelerated and Porosimetry System 2010 (ASAP 2010) from Micromeritics Inc.]. The commercial AC as control sample was purchased from K D Technology Sdn Bhd in powder form. *Table 3* lists its specifications. The MB purchased from Aldrich Chemical GmbH, Munich, Germany was used as an adsorbate in adsorption studies. The MB, chemical formula = C_{16} $H_{18}N_3CIS$, MW = 319.85 g mol^{-1}, λ_{max} = 668 nm.

Production of AC from Oil Palm Biomass

Production of biochar via pyrolysis. The oil palm biomass samples were dried at 105°C for 24 hr. The dried samples were then grinded and sieved. The fraction with particle diameter in the range of 2.0 mm was selected for the experiments. Both pyrolysis and activation process were conducted in

TABLE 1. PROXIMATE AND ULTIMATE ANALYSES OF OIL PALM BIOMASS

Oil palm biomass	Proximate analysis (wt%)				Ultimate analysis (wt%)				
	Fixed carbon	Moisture	Ash	Volatile matter	C	H	N	S	O
Empty fruit bunch (EFB)	19.1+0.7	9.2+0.8	2.1+0.9	69.6+0.9	52.37	7.47	1.78	ND	38.38
Palm kernel shell (PKS)	16.9+1.1	7.6+0.7	3.7+1.2	71.8+0.9	44.83	5.67	0.92	ND	48.58
Mesocarp fibre (MF)	12.0+0.0	9.3+0.4	7.2+0.9	71.5+0.6	47.05	3.19	1.43	ND	48.33

Note: C - carbon. N - nitrogen. O - oxygen. ND - not determined.
H - hydrogen. S - sulphur.

TABLE 2. SURFACE CHARACTERISTIC OF OIL PALM BIOMASS

Oil palm biomass	BET Surface area (m^2 g^{-1})	Total pore volume (cm^3 g^{-1})	Pore size (nm)
Empty fruit bunch (EFB)	231.52	0.1890	3.67
Palm kernel shell (PKS)	205.86	0.3707	3.43
Mesocarp fibre (MF)	239.50	0.3509	4.10

Note: BET - Brunauer-Emmet-Teller.

TABLE 3. SPECIFICATIONS OF COMMERCIAL ACTIVATED CARBON

Parameter	Typical value
Iodine number, mg g^{-1}	950-1150
Ash content, %	5 maximum
Apparent density, g cm^{-3}	0.42-0.52
Moisture, %	5 maximum
pH	9-11
Particle size distribution, %	90
BET surface area, m^2 g^{-1}	1 088

Note: BET - Brunauer-Emmet-Teller.

a horizontal quartz tube placed in a tube furnace as shown in *Figure 1*.

The biochar of oil palm biomass was prepared using the optimum conditions as described in Foo and Hameed (2011a). The dried EFB (20 g), was loaded onto a crucible, then heated up at 10°C min^{-1} to the desired temperature (700°C) for 2 hr under N_2 flow (150 cm^3 min^{-1}). The sample was allowed to cool to room temperature in an inert atmosphere. This pyrolysed sample devoted as biochar ($BEFB_o$) was utilised as precursors for preparing the AC. PKS and MF were subjected to the same procedure to produce the respective biochar, coded as $BPKS_o$ and BMF_o.

Physical Activation in Production of AC

The 10 g of the respective optimised biochar ($BEFB_o$, BMF_o, $BPKS_o$) was placed into a horizontal quartz tube furnace under N_2 flow (200 cm^3 min^{-1}) (*Figure 1*). The furnace was purged with N^2 for 15 min prior to the activation process. The temperature was increased at 10°C min^{-1} under flowing N_2 until the desired activation temperature 900°C was reached, after which the N_2 flow was switched to CO_2 (100 cm^3 min^{-1}). The activation temperature and CO_2 flow rate were kept constant for 30 min and upon finishing, the respective AC sample was cooled down under N_2 flow (100 cm^3 min^{-1}).

Characterisation of Produced AC

The scanning electron microscope (SEM) analysis of AC was recorded using Hitachi S-3400N. The physical properties of the produced AC were obtained by measuring their nitrogen adsorption-desorption isotherms at -196°C in an Accelerated and Porosimetry System (ASAP 2010, Micromeritics USA). Three steps were adopted in measuring the nitrogen adsorption-desorption isotherms. These include the dehydration of sample followed by degassing of sample under low vacuum pressure and nitrogen gas adsorption. The Brunauer-Emmet-Teller (BET) S_{BET} was calculated using the multilayer coverage adsorption data in a relative pressure range from 0.05 to 0.20 (Gregg and Sing, 1982). The total pore volume (V_T) was assessed by converting the amount of nitrogen gas adsorbed (expressed in cm^3 g^{-1} at STP) at relative pressure ≈ 0.97 to the volume of liquid adsorbate. The pore size distribution was calculated based on differential pore volume of Barrett-Joyner-Halenda (BJH) adsorption/desorption (Gregg and Sing, 1982).

Adsorption Equilibrium Isotherm Studies

About 0.1 g of the respective AC was added into a 100 ml MB solution at six different initial concentrations (150, 250, 300, 400, 500 and 600 mg $litre^{-1}$) in 250 ml conical flasks. The conical flasks were covered with aluminium foil to avoid the evaporation of MB from the solution. Deionised water was used to prepare the stock of MB solutions. An adsorption process was carried out at ambient temperature for 24 hr in a shaker operating at 150 rpm. The solutions were then filtered by a vacuum and the clarified solutions were analysed using a UV/Vis double beam spectrophotometer

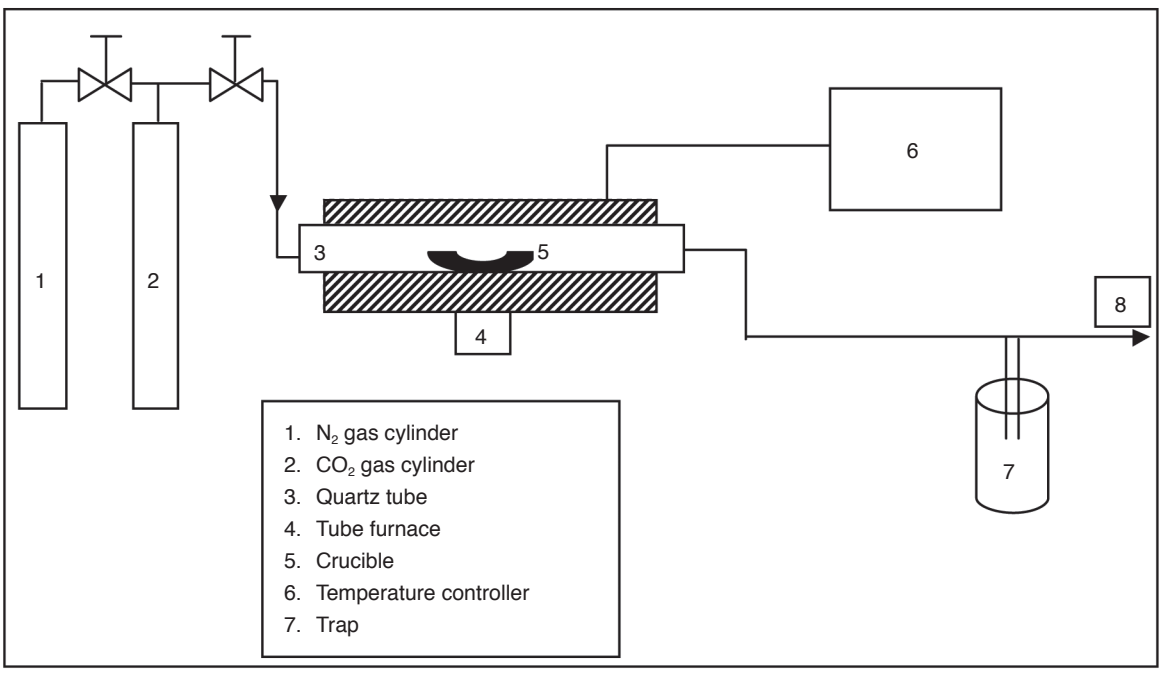

Figure 1. A schematic diagram of the experimental set-up.

at a maximum wavelength of 663 nm. The amount of MB adsorbed onto the AC was measured by subtracting the remaining concentrations of the MB solution from the initial concentration. The final concentration of the solution was then determined from the calibration curve.

The dye concentration at equilibrium, q_e (mg g^{-1}), was calculated as in Equation (1)

$$q_e = \frac{V(C_o - C_e)}{1000\ m} \qquad \text{Equation (1)}$$

where C_o (mg dm^{-3}) is the initial dye concentration in liquid phase, C_e (mg dm^{-3}) is the dye concentration in liquid phase at equilibrium, V (dm^{-3}) is the total volume of dye solution and m (g) is the mass of adsorbent (AC).

Adsorption Kinetics Studies

AC prepared from BEFB was evaluated as an adsorbent in MB dye adsorption study. Equilibrium isotherms of MB to EFB AC were analysed using two models, namely Langmuir and Freundlich. An accurate equilibrium isotherm and its isotherm constant can be determined through linear regression and the method of least squares, respectively from Equation (2) to Equation (5).

The Langmuir isotherm [Equation (2)] implies the formation of monolayer coverage of adsorbate on the surface of the adsorbent.

$$q_e = \frac{K_L C_e}{1+\alpha_L C_e} \qquad \text{Equation (2)}$$

$$\frac{C_e}{q_e} = \frac{\alpha_L C_e}{K_L} + \frac{1}{K_L} \qquad \text{Equation (3)}$$

where q_e is the dye concentration at equilibrium, K_L ($dm^3\ g^{-1}$) and α_L ($dm^3\ mg^{-1}$) are Langmuir isotherm constants. By plotting $[(C_e)/(q_e)]$ *vs*. C_e [Equation (3)], the Langmuir constants K_L and α_L can be obtained from the slope and intercept of the plot, respectively. The ratio of K_L/α_L gives the monolayer saturation capacity.

The Freundlich isotherm [Equation (4)] is an empirical equation employed to describe heterogeneous systems. It describes reversible adsorption and is not restricted to the formation of monolayer.

$$q_e = K_F C_e^{1/n} \qquad \text{Equation (4)}$$

$$\log q_e = \log K_F + 1/n \log C_e \qquad \text{Equation (5)}$$

where K_F ($dm^3\ g^{-1}$) is the Freundlich constant and 1/n is the heterogeneity factor. A plot of log q_e *vs*. log C_e permits the determination of 1/n and K_F from the slope and intercept.

Application of AC in POME

The final discharge of POME samples were collected from a palm oil mill with an average quality as follows: 154 ppm biochemical oxygen demand (BOD_3), 3238 ppm chemical oxygen demand (COD), 912 ppm suspended solid (SS) and 11700 Pt Co colour. In the batch treatment process for adsorption study, the effects of different dosages of AC (0.5, 1, 2, 3, 5, 6, 7, 8 and 9 w/v%) on BOD_3, COD, SS and colour at 150 rpm shaking speed in contact with POME for 24 hr at ambient temperature were studied.

RESULTS AND DISCUSSION

Surface Characteristics of AC

Table 4 shows the surface properties of biochar from different oil palm biomass (EFB, MF, PKS) at the previously reported optimum pyrolysis conditions (Foo and Hameed, 2011b). The biochar BEFBo showed the highest S_{BET} among the biochar produced. *Figure 2* shows the nitrogen adsorption isotherm of one of the biochar $BEFB_o$ at the optimised pyrolysis conditions *i.e.* 700°C for 2 hr with heating rate of 10°C min^{-1}. The shapes of the isotherms of all the biochar samples ($BEFB_o$, BMF_o, $BPKS_o$) were similar, *i.e.* type IV isotherm according to the Brunauer, Deming, Deming and Teller (BDDT) classification with the hysteresis loops corresponding to type H3 of the IUPAC classification (Sing and Williams, 2004). The oil palm biomass-derived biochar showed much lower S_{BET} which was indicative of a mesoporous material with a lower adsorption capability. The physical activation, as in this study, would potentially increase its S_{BET} and porosity.

The AC produced from $BEFB_o$ at various activation temperatures (*Table 5*) showed that the optimum surface activity and porosity characteristic were achieved at 800°C for 30 min giving $BEFB_o$ AC800 the maximum S_{BET} of 937 $m^2\ g^{-1}$. This indicated that the activation temperature was crucial in AC production. All AC were successfully altered from their mesoporous originalities to

TABLE 4. SURFACE PROPERTIES OF BIOCHAR PREPARED FROM DIFFERENT OIL PALM BIOMASS

Biochar source	Surface area (S_{BET}) ($m^2\ g^{-1}$)	Total pore volume ($cm^3\ g^{-1}$)	Pore size (nm)
Empty fruit bunch ($BEFB_o$)	347.043	0.4482	5.16
Mesocarp fibre (BMF_o)	217.347	0.3707	4.57
Palm kernel shell ($BPKS_o$)	205.859	0.1890	4.25

Note: $BEFB_o$, BMF_o, $BPKS_o$ - the respective biochar produced at optimum condition: temperature – 700°C; time – 2 hr; heating rate – 10°C min^{-1}

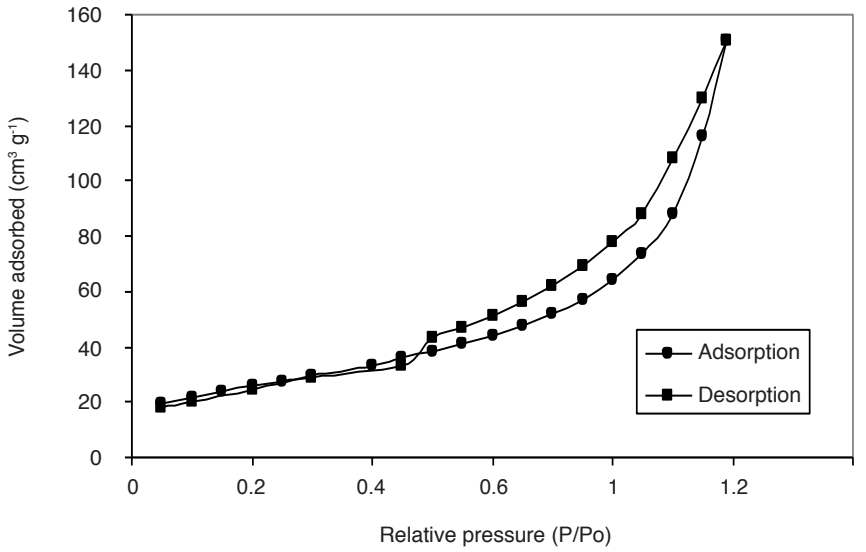

Figure 2. Example of nitrogen adsorption isotherm of palm-based biochar, $BEFB_o$ at -196°C.

TABLE 5. SURFACE PROPERTIES OF ACTIVATED CARBON (AC) PREPARED FROM EMPTY FRUIT BUNCH (EFB)-BASED BIOCHAR ($BEFB_O$)

AC sample	Surface area (S_{BET}) ($m^2\ g^{-1}$)	Microporous surface area (S_{MICRO}) ($m^2\ g^{-1}$)	Mesoporous surface area (S_{MESO}) ($m^2\ g^{-1}$)	Total pore volume (V_{MICRO}) ($cm^3\ g^{-1}$)	Pore size (nm)
$BEFB_o$ AC500	93	27	66	0.0183	3.5
$BEFB_o$ AC600	109	76	33	0.1064	2.9
$BEFB_o$ AC700	405	283	122	0.2107	3.1
$BEFB_o$ AC800	937	871	66	0.2837	2.0
$BEFB_o$ AC900	76	63	13	0.0149	2.5

Note: $BEFB_o$ - biochar derived from EFB at optimum pyrolysis condition.
ACxxx - AC produced at activation temperature xxx°C.

microporous characteristics with almost similar pore diameter, within the narrow range from 2.0 to 3.5 nm. The $BEFB_o$ AC800 was dominated with micropores which accounted for 93% of its total SBET. The degree of microporosity was found to increase steadily with the decrease in pore diameter. The adsorption-desorption isotherm of the $BEFB_o$ AC800 (*Figure 3*) showed a typical Type 1 isotherm of BDDT classification (Barret *et al*., 1951). Unlike $BEFB_o$, its adsorption capability increased rapidly at a low relative pressure in the range of 0.0-0.2, and stagnant after that at pressure >0.2.

In *Figure 4*, the pore structures in $BEFB_o$ AC800 were mainly micropores (93%) with an average pore size of 20Å (2 nm). The molecular diameter of MB (≈ 0.8-0.9 nm) was far smaller than the pore size of $BEFB_o$ AC800 to allow for its penetration, thus adsorption of MB occured. These findings have confirmed that an effective adsorbent should exhibit a large volume of micropores.

In *Figure 5*, the surface topography of the raw EFB (A) was significantly different from that of $BEFB_o$ AC800 (B). The SEM showed that the surface of raw EFB was rough with lots of big particles and holes, while that of the $BEFB_o$ AC800 was carbonous with lots of micropores. It can be found that the $BEFB_o$ AC800 with the highest S_{BET} demostrated a well pronounced, uniform and highly porous structures, indicating a good possibility for the dyes to be trapped and adsorbed.

Adsorption Equilibrium Isotherms and Kinetics Studies

The sorption behaviour of MB onto $BEFB_o$ AC800 (*Table 6*) analysed using linear regression, suggested that Freundlich isotherm was the best fitted model in this study. It gave the highest consistent correlation coefficient, R^2 of >0.999, indicating that the model correlated well with the adsorption equilibrium data, also suggesting that the adsorption of MB on the AC was favourable. This suggested that some heterogeneity on the surfaces or pores of the AC played the role in MB adsorption.

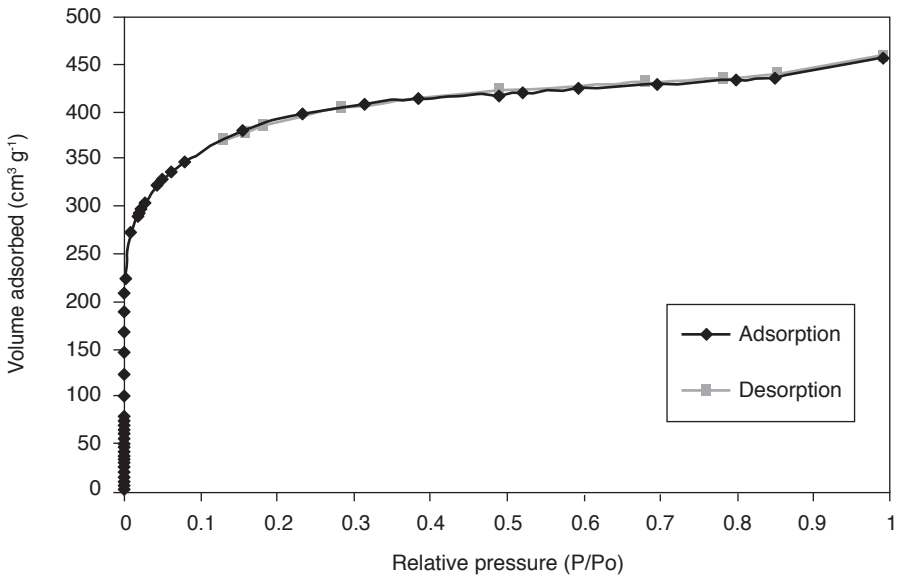

Note: $BEFB_o$ - biochar derived from empty fruit bunch (EFB) at optimum pyrolysis condition.
AC800 - activated carbon produced at optimum physical activation condition.

Figure 3. Nitrogen adsorption isotherm of $BEFB_o$ AC800.

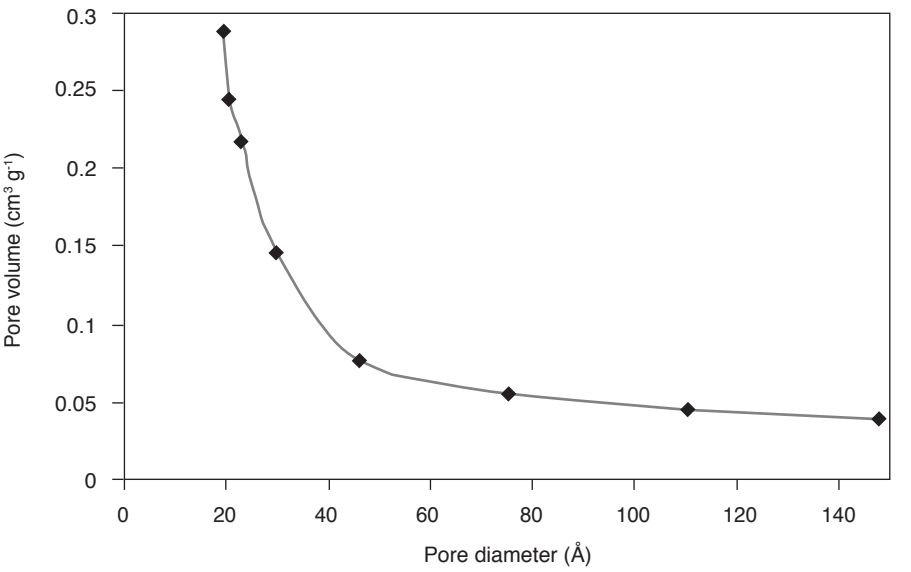

Figure 4. Pore size distribution of activated carbon (AC) prepared from empty fruit bunch (EFB)-based biochar ($BEFB_o$ AC800) at optimum conditions.

The Langmuir isotherm, on the other hand, was less fitted for MB sorption on $BEFB_o$ AC800 due to the inconsistent lower R^2. Nevertheless, the saturation capacities of the MB's monolayer sorption model as depicted in the Langmuir isotherm were found ranging from 277.8 to 333.3 mg g^{-1}. The Freundlich equation was more suitable when a change in the mechanism of adsorption with concentration was considered. The Langmuir equation is applied for homogenous surface while the Freundlich isotherm model assumed neither homogenous site energies nor limited levels of adsorption and can result from the overlapping patterns of several Langmuir-type adsorption phenomena occurring at different sites on complex adsrobents (Calace *et al*., 2002). The results agreed with the study carried out by previous researchers which reported that the Freundlich model gave a better fit than the Langmuir model on the adsorption of 2,4,6 – trichlorophenol using oil palm EFB-based AC (Tan *et al*. 2009). The study suggested that the resulting $BEFB_o$ AC could be potentially developed into an alternative adsorbent for wastewater treatment.

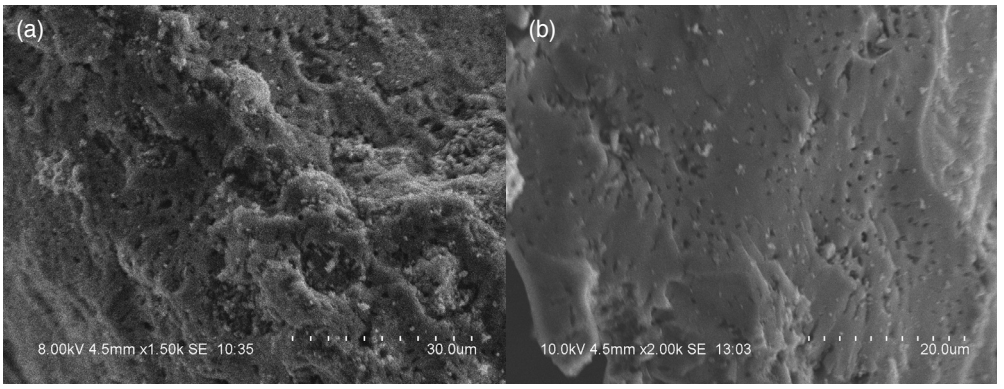

Figure 5. Scanning electron micrograph images of raw empty fruit bunch (EFB) fibres (a) and activated carbon (AC) prepared from empty fruit bunch (EFB)-based biochar ($BEFB_o$ AC800) at optimum conditions (b).

The influence of MB dye concentration, C_e (ranged from 0 to 60 mg $litre^{-1}$) on $BEFB_o$ AC was shown in *Figure 6*. The adsorption capacity (q_e) increased with increasing C_e from 50 mg g^{-1} to 420 mg g^{-1}, 150 mg g^{-1} to 550 mg g^{-1} and 150 mg g^{-1} to 580 mg g^{-1}, for $BEFB_o$ AC600, $BEFB_o$ AC700 and $BEFB_o$ AC800, respectively. The q_e of $BEFB_o$ AC800 correlated well with its maximum S_{BET} showing evidence in adsorbing MB onto the AC and removing it as a pollutant. However, once the adsorption of MB reached its maximum saturated point at equilibrium, the q_e would slow down even with further increase in C_e.

To compare, the adsorption capacity of $BEFB_o$ AC obtained in this study was larger than most of the other low-cost adsorbents deriving from agricultural wastes (*Table 7*), thus the $BEFB_o$ AC could be efficient in pollutant (dyes/organic matters) removal from wastewater. Its applicability in treating the wastewater of the palm oil milling process, *i.e.* POME is particularly of interest since POME is a highly organic-based material.

TABLE 6. ISOTHERM CONSTANTS FOR METHYLENE BLUE SORPTION ONTO ACTIVATED CARBON (AC) FROM EMPTY FRUIT BUNCH (EFB)-BASED BIOCHAR ($BEFB_O$) PREPARED AT DIFFERENT ACTIVATION TEMPERATURE

	$BEFB_o$ AC600	$BEFB_o$ AC700	$BEFB_o$ AC800
Langmuir			
$K_L/\dot{\alpha}_L$ (mg g^{-1})	277.8	312.5	333.3
$\dot{\alpha}_L$ (dm^3 mg^{-1})	0.7837	0.1236	0.5264
R^2	0.9995	0.9426	0.9658
Freundlich			
K_F (mg g^{-1})	0.5116	0.5135	0.4819
1/n	0.9914	0.9941	1.0021
R^2	0.9994	0.9998	0.9995

Note: $BEFB_o$ - biochar derived from EFB at optimum pyrolysis condition.
ACxxx - AC produced at activation temperature xxx°C.

Application of AC in POME Treatment

The $BEFB_o$ AC800 was further used in the tertiary POME treatment since it had the highest S_{BET}. In *Figure 7*, the concentrations of BOD_3, COD and SS of the treated POME dropped sharply with increasing of AC dosage at the beginning of POME treatment, afterwhich the reduction slowed down before reaching a maximum reduction at 9% (w/v) treatment dosage of AC. The reduction was 88%, 98% and 96%, respectively for a 24 hr treatment period (*Figure 7*). This trend was in agreement with the Langmuir equilibrium isotherm precisely comfirming that the adsorption of organic pollutants onto $BEFB_o$ AC800 had reached its saturation capacity midway down the treatment. The BOD_3, COD and colour adsorption capabilities of $BEFB_o$ AC800 as compared to that of the commercial AC were as shown in *Figures 8*, *9* and *10*, respectively. The results showed that the $BEFB_o$ AC800 was comparable with the commercial grade AC in treating POME.

CONCLUSION

The $BEFB_o$ AC produced from the pyrolysis and physical activation process was comparable to

TABLE 7. COMPARISON OF THE MAXIMUM DYE ADSORPTION CAPACITIES (q_e) OF THE EMPTY FRUIT BUNCH-BASED ACTIVATED CARBON (AC) AND OTHER ACS PREPARED FROM AGRICULTURAL WASTES

Source of AC	Adsorption q_e capacity, (mg g^{-1})	References
Date stone	28.57	Sekirifa *et al*. (2013)
Corn cob	187.67	Song *et al*. (2013)
Sludge paper mil	130.69	Li *et al*. (2011)
High ash raw bagasse	391.00	Valix *et al*. (2004)
Palm kernel shell	311.72	Jumasiah *et al*. (2005)
Empty fruit bunch	333.33	This study

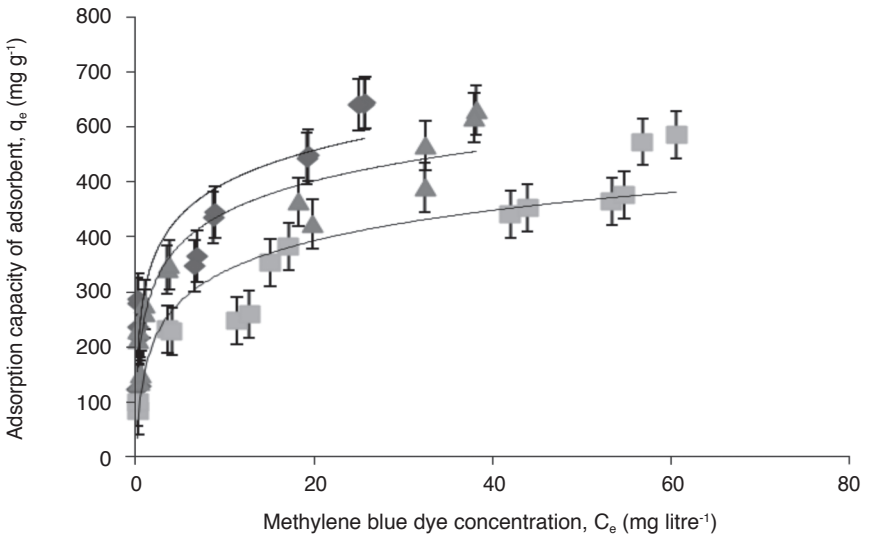

Note: $BEFB_o$ - biochar derived from empty fruit bunch (EFB) at optimum pyrolysis condition.
ACxxx -AC produced at activation temperature xxx°C.

Figure 6. Equilibrium curves for sorption of methylene blue onto $BEFB_o$ AC.

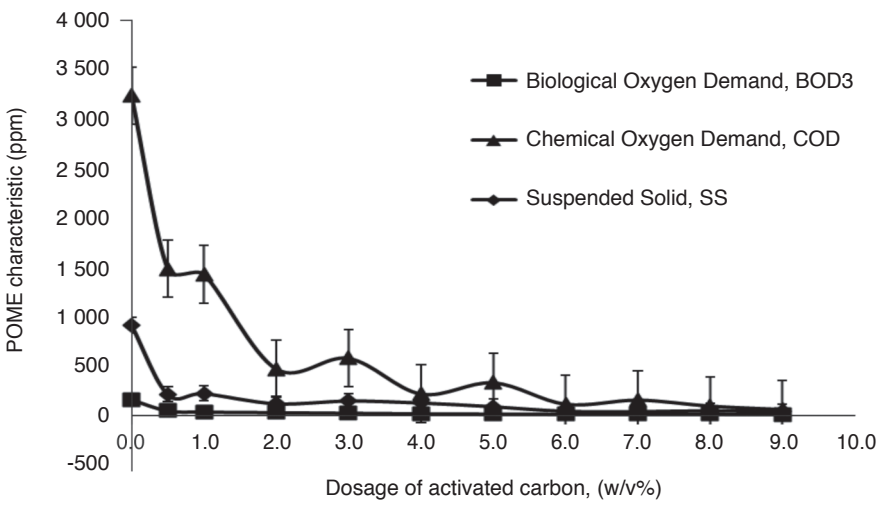

Figure 7. The characteristics of palm oil mill effluent after treatment with empty fruit bunch-based activated carbon ($BEFB_o$ AC800) at different dosage (batch process).

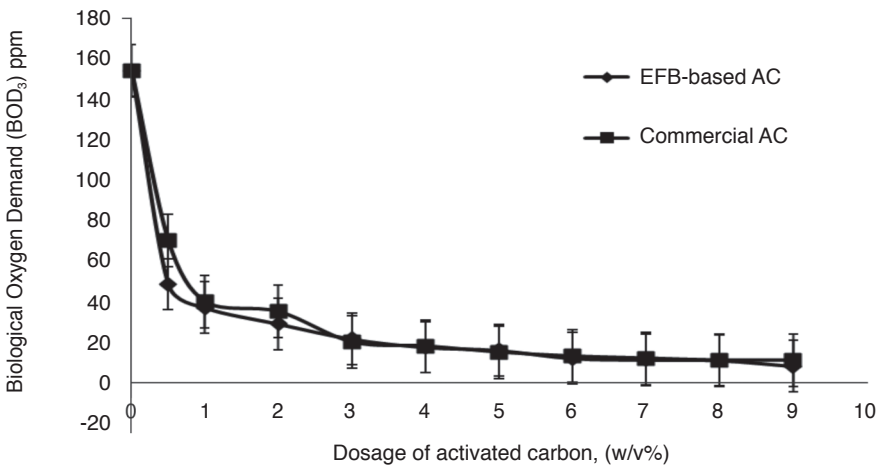

Figure 8. Adsorption capability between empty fruit bunch-based activated carbon ($BEFB_o$ AC800) and commercial activated carbon(AC) in BOD_3 of palm oil mill effluent.

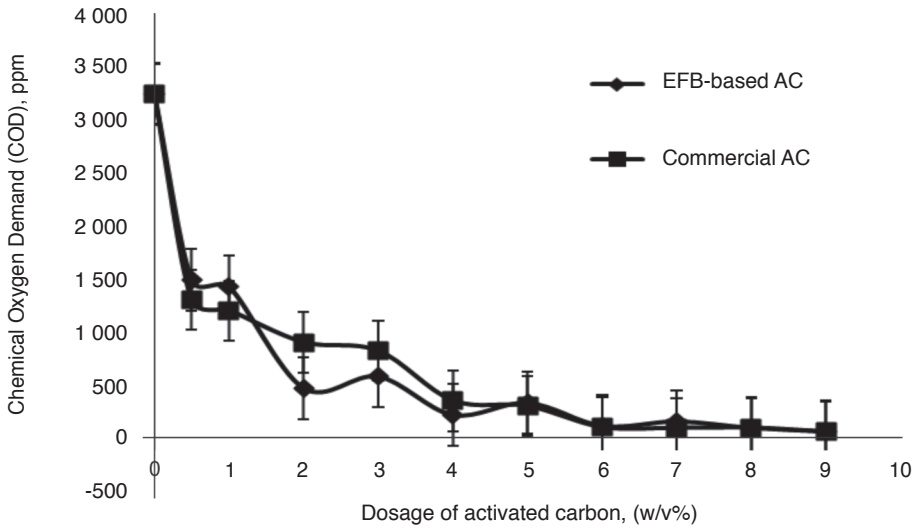

Figure 9. Adsorption capability between empty fruit bunch-based activated carbon ($BEFB_o$ AC800) and commercial activated carbon (AC) in Chemical Oxygen Demand (COD) of palm oil mill effluent.

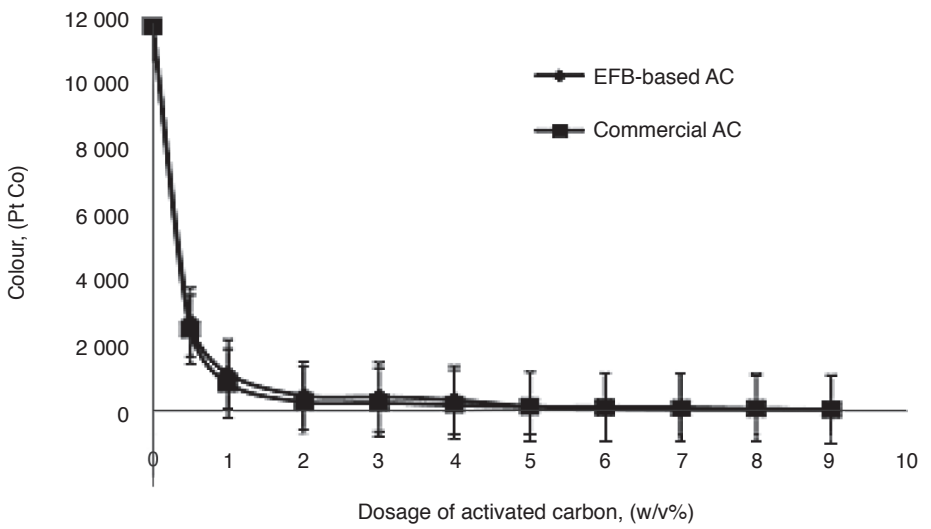

Figure 10. Adsorption capability between empty fruit bunch-based activated carbon ($BEFB_o$ AC800) and commercial activated carbon (AC) in colour of palm oil mill effluent.

the commercial grade AC, in terms of the S_{BET} and the q_e. The $BEFB_o$ AC800 having its S_{BET} of 937 $m^2 g^{-1}$ was found performing the highest q_e for MB. The physical activation process was successfully optimised to develop $BEFB_o$ AC dominated with microporous surfaces that could increase the absorptive capability of MB. Similarly, the $BEFB_o$ AC was found able to reduce the organic pollutants and colored component with low dosages and short treatment time which at 9% (w/v) and 24 hr, respectively, of POME in its final discharge into a waterway.

ACKNOWLEDGEMENT

The author would like to thank the Director-General of MPOB for permission to publish this article. Thank are also due to the staff of the Biodisel Technology Group, Engineering and Processing Division, MPOB for their assistance.

REFERENCES

ADINATA, D; DAUD, W M A W and AROUA, M K (2007). Preparation and characterization of activated carbon from palm shell by chemical activation with K_2CO_3. *J. Bioresource Technology, 98*: 145-149.

ALAM, M Z; AMEEM, E S; MUYIBI, S A and KABBASHI, N A (2009). The factors affecting the performance of activated carbon prepared from oil palm empty fruit bunches for adsorption of phenol. *J. Chemical Engineering, 155*: 191-198.

AMOSA, M K (2015). Process optimisation of Mn and H_2S removals from POME using an enhanced empty fruit bunch (EFB)-based adsorbent produced by pyrolysis. *J. Environmental Nanotechnology, Monitoring and Manangement, 4*: 93-105.

ARENAS, E and CHEJNE, F (2000). The effect of the activating agent and temperature on the porosity development of physically activated coal chars. *J. Carbon, 42*: 2451-2455.

ASTIMAR, A A and DERAMAN, M (2013). Pore structure of carbon granules prepared from slow pyrolysis of oil palm empty fruit bunch fibres. *J. Oil Palm Res. Vol. 25*: 216-227.

AYGUN, A; KARAKAS, S Y and DUMAN, I (2003). Production of granular activated carbon from fruit stones and nutshells and evaluation of their physical, chemical and adsorption properties, micropore, mesopore. *J. Materials, 66*: 189-195.

BANAT, F; AL-ASHEH, S and AL-MAKHADMEH L (2003). Evaluation of the use of raw and activated date pits as potential adsorbents for dye containing waters. *J. Process Biochem., 39*: 192-202.

BARRET, E P; JAOYNER, L G and HALENDA, P P (1951). The determination of pore volume and area distributions in porous substances: computations from nitrogen isotherms. *J. Amer. Oil Chem. Soc., 73*: 373-380.

BOUCHELTA, C; MEDJRAM, M S; BERTRAND, O and BELLAT, J P (2008). Preparation and characterization of activated carbon from date stones by physical activation with steam. *J. Analytical and Applied Pyrolysis, 82*: 70-77.

CALACE, N; NARDI, E and PETRONIO, B M (2002). Adsorption of phenols by paper mills sludges. *J. Environmental Pollution, 118*: 315-319.

CEYHAN, A A; SAHIN, O; BAYTAR, O and SAKA, C (2013). Surface and porous characterization of activated carbon prepared from pyrolysis of biomass by two-stage procedure at low activation temperature and it's the adsorption of iodine. *J. Analytical and Applied Pyrolysis, 104*: 378-383.

DAUD, W M A W; ALI, W S W and SULAIMAN, M Z (20000. The effects of carbonization temperature on pore development in palm-shell-based activated carbon. *J. Carbon, 38*: 1925-1932.

DEVI, R; SINGH, V and KUMAR, A (2008). COD and BOD reduction from coffee processing wastewater using avocado peel carbon. *J. Bioresource Technol, 99*: 1853-1860.

FOO, K Y and HAMEED, B H (2011a). Preparation of oil palm (*Elaeis*) empty fruit bunch activated carbon by microwave-assisted KOH activation for the adsorption of methylene blue. *Desalination, 275*: 302-305.

FOO, K Y and HAMEED, B H (2011b). Microwave-assisted preparation of oil palm fibre activated carbon for methylene blue adsorption. *J. Chemical Engineering, 166*: 792-795.

FREEL, B; LIAW, G and FERGUSON, C (2004). Process for producing activated carbon. Patent No. US 2004/0097369 A1.

GREGG, S J and SING, K S W (1982). *Adsorption, Surface Area and Porosity*. Academic Press, London. p. 473.

GUEYE, M; RICHARDSON, Y; KAFACK, F T and BLIN, J (2014). High efficiency activated carbons from African biomass residues for the removal of chromium(VI) from wastewater. *J. Environmental Chemical Engineering, 2*: 273-281.

GUO, J and LUA, A C (2001). Preparation and characterization of activated carbons from oil-palm stones for gas-phase adsorption. *J. Colloids and Surfaces, 179*: 151-162.

GUO, J and LUA, A C (2002). Microporous activated carbons prepared from palm shell by thermal activation and their application to sulphur dioxide adsorption. *J. Colloid and Interface Science, 251*: 242-247.

GUO, J; WONG, X S; CHEN, Y L and LUA, A C (2005). Adsorption of NH_3 onto activated carbon prepared from palm shells impregnated with H_2SO_4. *J. Colloid and Interface Science, 281*: 285-290.

GUO, J; LUO, Y; LUO, A C; CHI, R; CHEN, Y; BAO, X and XIANG, S (2007). Adsorption of hydrogen sulphide (H_2S) by activated carbons derived from oil palm shell. *Carbon, 45*: 330-336.

HAMEED, B H; TAN, I A W and AHMAD, A L (2009). Preparation of oil palm empty fruit bunch-based activated carbon for removal of 2,4,6-trichlorophenol: optimization using response surface methodology. *J. Hazardous Materials, 164*: 1316-1324.

HAMEED, B H; DIN, A T and AHMAD, A L (2007). Adsorption of methylene blue onto bamboo-based activated carbon: kinetics and equilibrium studies. *J. Hazardous Materials, 141*: 819-825.

HAYASHI, J; HORIKAWA, T; TAKEDA, I; MUROYAMA, K and ANI, F N (2002). Preparing

activated carbon from various nutshells by chemical activation with K_2CO_3. *J. Carbon, 40*: 2381-2386.

HU, Z and SRINIVASAN, M P (2000). Mesoporous high-surface-area activated carbon. *Microporous and Mesoporous Materials, 43*: 267-275.

ISMADJI, S; SUDARYANTO, Y; HARTONO, S B; SETIAWAN, L E K and AYUCITRA, A (2005). Activated carbon from char obtained from vacuum pyrolysis of teak sawdust: pore structure development and characterization. *J. Biosource Technology, 96*: 1364-1369.

JUMASİAH, A; CHUAH, T G; GİMBON, J; CHOONG, T S Y and AZNİ, I (2005). Adsorption of basic dye onto palm kernel shell activated carbon: sorption equilibrium and kinetics studies. *J. Desalination, 186*: 57-64.

LOH, S K (2016). The potential of the Malaysian oil palm biomass as a renewable energy source. *J. Energy Conversion and Management.* http://dx.doi.org/10.1016/jenconman. 2016.08.081.

LI, W H; YUE, Q Y; GAO, B Y; WANG, W J; QI, Y F; ZHAO, Y Q and LI, Y J (2011). Preparation of sludge-based activated carbon made from paper mill sewage sludge by steam activation for dye treatment. *J. Desalination, 278*: 179-185.

MPOB (2015). *Malaysian Oil Palm Statistic 2015*. 35th Edition. MPOB, Bangi. p. 28.

MALIK, P K (2004). Dye removal from wastewater using activated carbon developed from sawdust: Adsorption equilibrium and kinetics. *J. Hazard Matter, 113*: 81-88.

MD ARSHAD, S H; NGADI, N; ASTIMAR, A A; AMIN, N S; JUSOH, M and WONG, S (2016). Preparation of activated carbon from empty fruit bunch for hydrogen storage. *J. Energy Storage, 8*: 257-261.

MASOUD, M S; EL-SARAF, W M; ABDE-HALIM, A M; MOHAMED, E A and HASSAN, H M I (2016). Rice husk and activated carbon for waste treatment of El-Mex Bay, Alexandria Coast, Egypt. *Arabian J. Chemistry, 9*: 1590-1596.

MICHAEL, J A (1995). Process for charcoal production from woody and herbaceous plant material. Patent No. US 5,435,983.

MUBARAK, N M; SAHU, J N; ABDULLAH, E C and JAYAKUMAR, N S (2016). Palm oil empty fruit bunch based magnetic biochar composite comparison for synthesis by microwave-assisted and conventional heating. *J. Analytical and Applied Pyrolysis, 120*: 521-528.

NOR FAIZAH, J; ASTIMAR, A A; WAHAB, N A; WAN HASAMUDIN, W H and NAHRUL, H Z (2017). Application of palm kernel shell activated carbon for the removal of pollutant and color in palm oil mill effluent treatment. *J. Earth, Environment and Health Sciences, 2*: 15-20.

NUNES, A A; FRANCA, A S and OLIVIERA, L S (2009). Activated carbon from waste biomass: an alternative use for biodiesel production solid residues. *J. Biosource Technology, 100*: 1786-1792.

OMAR, R; IDRIS, A; YUNUS, R; KHALID, K and AIDA ISMA, M I (2011). Characteristic of empty fruit bunch for microwave-assisted pyrolysis. *J. Fuel, 90*: 1536-1544.

OSMAN, N B; SHAMSUDDIN, N and UEMURA, Y (2016). Activated carbon of oil palm empty fruit bunch (EFB): core and shaggy. *Procedia Engineering, 148*: 758-764.

SEKIRIFA, M L; MAHFOUD, H M; PALLIER, S; BAAMEUR, L; RICHARD, D and AL-DUJAILI, A H (2013). Preparation and characterization of an activated carbon from a date stones variety by physical activation with carbon dioxide. *J. Analytical and Applied Pyrolysis, 99*: 155-160.

SONG, M; JIN, B; XIAO, R; YANG, L; WU, Y; ZHONG, Z and HUANG, Y (2013). The comparison of two activation techniques to prepare activated carbon from corn cob. *J. Biomass and Bioenergy, 48*: 250-256.

SING, K S W and WILLIAMS, R T (2004). Physisorption hysteresis loop and the characterization of nanoporous materials. *Adsorption Science and Technology, 22*: 772-782.

SITI HADJAR, M A; ASTIMAR, A A; NORZITA, N and NORAISHAH, S A (2012). Phenol adsorption by activated carbon of different fibre size derived from empty fruit bunches. *J. Oil Palm Res. Vol. 24*: 1524-1532.

TAN, I A W; AHMAD, A L and HAMEED, B H (2009). Adsorption isotherms, kinetics, thermodynamics and desorption studies of 2,4,6-trichlorophenol on oil palm empty fruit bunch-based activated carbon. *J. Hazardous Materials, 164*: 473-482.

TAN, I A W; AHMAD, A L and HAMEED, B H (2008). Enhancement of basic dye adsorption uptake from aqueous solutions using chemically modified oil palm shell activated carbon. *J. Colloids and Surfaces, 318*: 88-96.

TAY, T; UCAR, S and KARAGÖZ, S (2009). Preparation and characterization of activated carbon from waste biomass. *J. Hazardous Materials, 165*: 481-485.

TIRYAKI, B; YAGMUR, E; BANFORD, A and AKTAS, Z (2014). Comparison of activated carbon produced from natural biomass and equivalent chemical compositions. *J. Analytical and Applied Pyrolysis, 105*: 276-283.

TREVIÑO-CORDERO, H; JUÁREZ-AGUILAR, L G; MENDOZA-CASTILLO, D I; HERNÁNDEZ-MONTOYA, V; BONILLA-PETRICIOLET, A and MONTES-MORÁN, M A (2013). Synthesis and adsorption properties of activated carbon from biomass of *prunus domestica* and *jacaranda minosifolia* for the removal of heavy metals and dyes from water. *Industrial Crops and Products, 42*: 315-323.

VALIX, M; CHEUNG, W H and MCKAY, G (2004). Preparation of activated carbon using low temperature carbonization and physical activation of high ash low raw bagasse for acid dye adsorption. *J. Chemosphere, 56*: 493-501.

YACOB, A R; MAJID, Z A; DASRIL, R S D and INDERAN, V (2008). Comparison of various sources of high surface area carbon prepared by different types of activation. *The Malaysian J. Analytical Sciences, 12*: 264-271.

ZAHRIM, A Y; RACHEL, F M; MENAKA, S; SU, S Y; MELVIN, F and CHAN, E S (2009). Decolorisation of anaerobic palm oil mill effluent via activated sludge-granular activated carbon. *J. World Apply Science, 5*: 126-129.